Titanium Dioxide (TiO_2) Doping Copper (Cu) with Annealing Temperature Variation as Photoanode for Dye-Sensitized Solar Cells (DSSC)

Enna Hasna Ainun Nuurul Ma'rifah[1*], *Agus* Supriyanto[1†], *Tika* Paramitha[2‡], *Hendri* Widiyandari[1], *Agus* Purwanto[2], and *Harry* Kasuma Kiwi Aliwarga[3]

[1]Physics Department Sebelas Maret University Surakarta, Indonesia
[2]Chemical Engineering Department Sebelas Maret University Surakarta, Indonesia
[3]UMG Idealab Jakarta, Indonesia

Abstract. Cu-doped Titanium Dioxide (TiO2) has been widely used as a DSSC photoanode material. The annealing temperature affects the structural analysis and optical properties of DSSC photoanodes. Structural analysis showed that the crystal size increased with increasing annealing temperature. The XRD results showed that the sample formed an anatase phase at annealing temperatures of 300°C and 400°C, while at 450°C and 500°C there was an anatase-rutile mixed phase. The results of SEM morphology data obtained average particle diameters for CT300, CT400, CT450, and CT500 materials were 23.87 µm, 32.54 µm, 33.38 µm, and 37.63 µm respectively. UV-Vis testing shows absorbance in the ultraviolet region at 350-400 nm. Increasing the annealing temperature decreases the absorbance. The efficiency of DSSC compared to undoped materials is 0.44% to 0.71% in samples with an annealing temperature of 300°C which is the sample with the highest efficiency. The efficiency value decreased with increasing annealing temperature.

1 Introduction

The need for energy has rapidly increased through technological growth. Solar cells are a solution that offers renewable energy that can convert solar energy into electrical energy. Solar energy has a broad potential as an electrical resource with infinite power, universal, and renewable for life [1]. The dye-sensitized solar cells (DSSC) work with principle that electron excitation due to light absorption events and charge separation. This solar cell was introduced in 1991 by Brian O'Regan and Michael Grätzel as low-cost solar cells [2]. This type has the potential to develop because has abundant materials, low cost, environmentally friendly, and can be fabricated quickly [3].

Photoanode is a crucial component at DSSC because it faces direct sunligh and must catch more solar irradiation. The number of photons which caught can influence the energy that can be produced from the conversion process. Photoanodes are usually comprise of metal oxide semiconductors such as TiO_2, ZnO, and SnO. TiO_2 material is often used in DSSC because it has good chemical stability, is affordable, and is non-toxic [4]. In its application, TiO_2 must have a large surface area to absorb more dyes. It can provide benefits through increased photon currents [5].

Recent research shows that Titanium (IV) Oxide, called TiO_2, has been a widely used photoanode material. TiO_2 has good chemical thermal stability, is non-toxic, and has greater availability at a cheaper cost. This material has a wide band gap of 3,02 eV for the rutile phase, 3,2 eV for the anatase phase, and 2,96 eV for the brookite phase. However, TiO_2 has a relatively active optical response that needs to be modify to improve its performance as a DSSC photoanode.

In terms of crystal structure, the anatase and rutile TiO_2 phases have a tetragonal crystal structure, while brookite has an orthorhombic crystal structure [6]. This difference in crystal structure caused by differences in distortion and the pattern of arrangement of the octahedral chains. The anatase structure has more considerable Ti-Ti distance than rutile that is 3.79 Å and 3.04 Å. Meanwhile, rutile has a Ti-Ti distance of 3.57 Å and 2.96 Å. Meanwhile, the distance between Ti-O in anatase is shorter than that of rutile, namely 1.93 Å and 1.98 Å in anatase, while that of rutile ranges between 1.95 Å and 1.99 Å [7]. The anatase phase with high electron mobility, low dielectric constant, and low density makes it suitable for DSSC. As for its chemical characteristics, TiO_2 has a refractive index n = 2.4 – 2.5 [8].

Doping is one of the modifications in the manufacture of working electrodes made from TiO_2 to improve DSSC performance. Transition metal groups has been widely used as doping materials, such as Nickel (Ni), Copper (Cu), and Silver (Ag). Titania with

* ennahasna27@gmail.com
† agusf22@staff.uns.ac.id
‡ tikaparamitha@staff.uns.ac.id

transition metal doping can improve the optical and electrical properties by changing the band gap. Therefore, adsorption geometry and dye adsorption on the TiO_2 surface will affect the open circuit voltage and solar cell efficiency. In addition, the oxygen vacancies formed after doping can increase the binding of dye molecules to the TiO_2 surface [3].

Copper (Cu) is a conductive metal with excellent thermal properties and has one electron on the outer shell that is capable of transitioning due to the small orbital energy levels. The electron configuration of Cu is [Ar] $3d^{10}4s^1$. The atomic radius of Cu^{2+}, which is 0.68 Å, is not much different from the atomic radius of Ti^{4+}, which is 0.61 Å, so Cu doping on TiO_2 can occur optimally and change its electronic density [9]. Copper doping reduces the surface area and band gap of TiO_2 so that more molecules can adsorbed onto the TiO_2 surface. Copper also has low toxicity and a lot of abundance in nature, so it has the potential to become a metal doping material [10]. Therefore, Cu can be inserted easily as doping of photoanode material.

Previous research shows the results can increase the electronic density optimally. Copper doping can decrease surface area and band gap energy TiO_2 so that the crystal size can be reduced and the number of adsorbed molecules can increase. Copper also less toxicity and great abundance to become a doping material potentially [10]. Although TiO_2 doping Cu has reported in other research papers, the influence of their annealing temperature at Cu-TiO_2 has not widely reported.

Annealing is a heating process held at that temperature for a specific time. Annealing form more optimal DSSC which affects the amount of grain and absorbance ability. It also can affects the current density [11]. The annealing temperature also increases the crystallinity without affecting the phase [12]. So, this research attempts to express the influence of TiO_2 doping Cu annealing temperature that applied for photoanode of DSSC. The role of annealing temperatures affects the characterization and optical properties.

This research examines the effect of annealing temperature on the manufacture of Cu-doped TiO_2 for photoanodes. In this study, the impact of annealing temperature on Cu-doped TiO_2 DSSC TiO_2 will observed including its structural, morphological, optical, and electrical properties.

2 Experimental

2.1 Synthesis of TiO_2 doping Cu

Titanium (IV) Oxide or TiO_2 doping Cu synthesized from 0,5 grams Titanium (IV) Oxide Sigma-Aldrich ≥99,5% solved with 3 ml ethanol and stirred at 500 rpm for 30 minutes at 30℃. The doping composition was made by solved Copper Sulfate Pentahydrate ($CuSO_4.5H_2O$) in distillate water to get 0,1 M $CuSO_4.5H_2O$ and stirred for 15 minutes with a speed of 500 rpm at 30℃. After that, the Copper solution was mixed with 3 ml of acetic acid and 30 ml of ethanol. And then stirred continuously for 15 minutes.

TiO_2 was mixed with doping solvent and stirred at 500 rpm for 3 hours. Then, the mixture was evaporated in the oven at 100 for 12 hours to evaporate the solvent. Materials TiO_2 doping Cu varied in the annealing temperature that is 300℃, 400℃, 450℃, and 500℃. All samples is CT300, CT400, CT450, and CT500.

2.2 Preparation of Photoanode

The slurry was made from TiO_2 doping Cu materials prepared with mixed 0,25 grams powder into 2 ml ethanol and stirred at 350 rpm for 2 hours. We used cleaned FTO (Fluorine Tin Oxide) conductive glass as substrate with size 2 cm ×2 cm. The active area is 0,5 cm ×0,5 cm. The FTO glass prepared by cleaning it in ultrasonic stirrer with alcohol 70% and aquadest for 30 minutes each.

The prepared slurry was deposited onto the FTO glass surface by spin coater with a speed of 3000 rpm for 30 seconds for each drop. The coating repeated for up to 3 drops. The sample DSSC for UV-visible spectroscopy made with the same method at FTO substrate size 2 cm ×3 cm onto active are 1 cm ×1 cm. Then, the photoanode thin layer was annealed at 450℃ for 30 minutes in the furnace. Then, the photoanodes were soaked in the 0,3 mM dye N719 for 24 hours and then washed with ethanol after they were finished.

2.3 Fabrication of DSSC

This research used a platina layer as counter electrode. The photoanode and counter electrode arranged like a sandwich with the two active areas in contact each other. The arrangement clamped with paper clips at both ends. The Mosalyte electrolyte solution injected using an injector micropipette until the active area of photoanode and working electrode were moistened with electrolyte. The samples were then subjected to a current-voltage (I-V) test to determine the electrical characteristics of the DSSC.

2.4 Characterization

The crystal structure of TiO_2 doping Cu materials measured by X-Ray Diffraction (XRD) D8 Advance Diffractometer Bruker USA with Cu- radiation. The surface morphology of the materials investigated using Scanning Electron Microscopy (SEM) Quanta 250/450/650 with magnification up to 20000x. The FTIR Shimadzu used to analyze the group bonds formed in the sample. The absorption of samples TiO_2 doping Cu thin layer was measured with *Double Beam Spectrophotometer* UV-1800 to record absorbance from the photoanode. DSSC samples tested with Keithley I-V 2602A to measure electrical quantities and determine DSSC efficiency values.

3 Results and Discussion

3.1 Structure Analysis

In this study, X-rays originate from Cu Kα anode material with a wavelength of 1.5406 Å. The characterization results are a diffraction pattern curve of 2 theta as the X axis and the intensity as the Y axis. The results of the XRD data shown in Figure 1.

The diffraction shows the XRD spectrum of the sample has been made in powder. The peak position and each intensity adjusted according to the standard diffraction pattern that is PDF No. 211272 for anatase TiO_2 and PDF No. 211276 for rutile TiO_2.

The TiO_2 material doped with Copper (Cu) did not experience a significant peak change compared to TiO_2 without doping. However, phase changes observed with different peaks present in each variation. In this study, anatase TiO_2 was used as evidenced by the XRD diffraction peaks. Cu-doped TiO_2 samples treated with annealing at 300°C had the anatase phase without any other phases. Peaks observed at different 2 tetha values which also corresponded to each crystal plane. This CT300 sample has peaks at 25.345˚ (101), 37.838˚ (004), 48.073˚ (200), 53.922˚ (105), 55.102˚ (211), 62.166˚ (213), 62.740˚ (204), 68.805˚ (116), 70.323˚ (220), 75.091˚ (215), and 76.081˚ (301) which are all peaks of the anatase phase. Meanwhile, the presence of Cu as a doping material observed at the peaks of 43.151˚ (111), 50.538˚ (200), and 74.923˚ (220) by studies showing the peaks of Copper at 43.28˚ (111), 50.40˚ (200), and 74.81˚ (220).

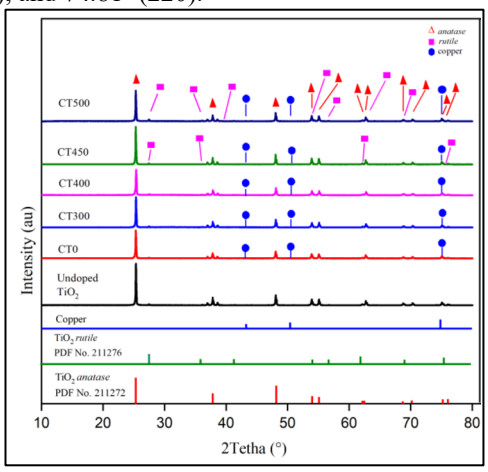

Fig. 1. Diffraction pattern of Cu-doped TiO_2 material with various variations of annealing temperature.

The same thing happened to Cu-doped TiO_2, which annealed at 400°C. The diffraction peak is the same as the diffraction peak in the CT300 sample. Thus, the annealing temperature treatment at 300°C and 400°C did not change the initial phase of TiO_2.

Sample of Cu-doped TiO_2 treated with annealing 450°C and 500°C have an additional peak of the rutile phase was observed. While the peaks of the rutile phase were observed at 27.456˚ (110), 36.091˚ (101), 62.869˚ (002), and 76.276˚ (202). In this variation, not all rutile peaks observed because the phase formed was in the form of an anatase-rutile mixed phase.

The highest annealing temperature variation, 500°C, showed the anatase-rutile mixed phase with more rutile peaks than CT450 sample. In comparison, the peaks of rutile observed at 27.457˚ (110), 36.092˚ (101), 41.247˚ (111), 54.038˚ (211), 56.660˚ (220), 62.859˚ (002), and 68.791˚ (301). The CT500 sample has more rutile peaks than the CT450 sample. It indicates that a mixed phase of anatase-rutile occurred. The changes in crystal structure and occurrence of mixed phases caused by the presence of oxygen vacancies, which controlled during particle growth as a function of annealing temperature.

The addition of Cu doping shifts the intense peak of TiO_2, as shown in Figure 2. The peak moved to the right from the specified database. This shift due to the dilation compared to the undoped sample indicates the insertion of other materials in the form of doping into the crystal lattice which affects the size of the crystal [13].

Crystal size, d, is obtained using the Debye Scherrer equation for the equation of Full Width at Half Maximum (FWHM), corresponding to the following equation 1.

$$d = \frac{K\lambda}{2B\cos\theta} \quad (1)$$

where d is the crystal size, λ is the diffraction wavelength, B is the FWHM value, θ is the diffraction angle, and K is a constant.

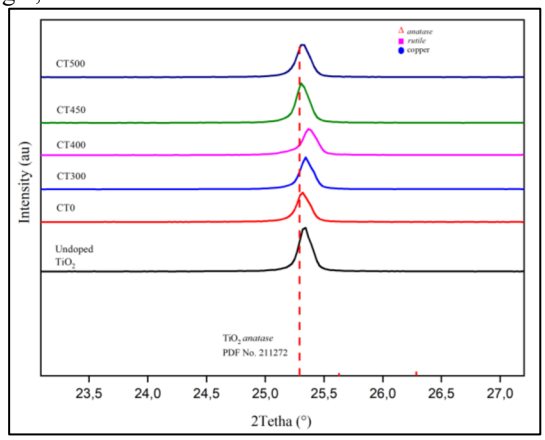

Fig. 2. Strong peak shift in the sample

The crystal size of CT300 is the smallest among other samples, namely 34.82 nm. While the size of CT400 increased to 35.96 nm and CT450 has a size of 43.54 nm. Meanwhile, CT500 was given the largest crystal size around 47.54 nm. It is also following the research which states that the crystal size increases with an increase in annealing temperature [14]. These results are also consistent with studies showing that the crystal size results of Cu-doped TiO_2 range from 10-40 nm [13]. It indicates that the crystallinity of the sample has increased with increasing annealing temperature [14].

3.2 Discussion for Practical Implementation and Future Challenges

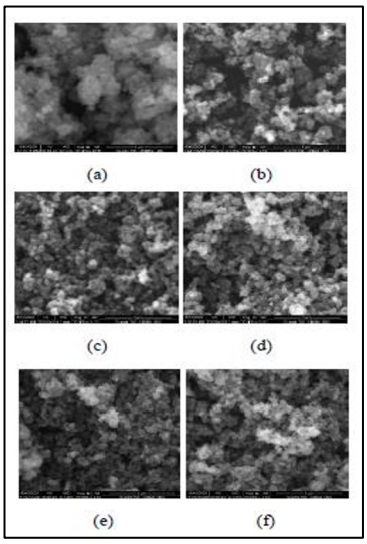

Fig. 3. Morphological results of samples using SEM magnification 20000x for samples a) undoped TiO_2, b) CT0, c) CT300, d) CT400, e) CT450, and f) CT500

The pure TiO_2 material does not undergo an annealing process so crystals do not form. The samples without annealing had agglomerations but the number of agglomerates was less than samples without doping. The addition of doping changes the morphology of the resulted material (Chahid et al., 2018). In the image, it is observed that the lighter-colored particles indicate other materials, namely in the form of Cu doping materials added to the sample. Based on these data, it found that the average particle diameters for the materials CT300, CT400, CT450, and CT500 were 23.87 µm, 32.54 µm, 33.38 µm, and 37.63 µm respectively. The largest diameter size owned by the CT500 sample with a particle size of 37.63 µm.

3.3 Chemical Bonding Analysis

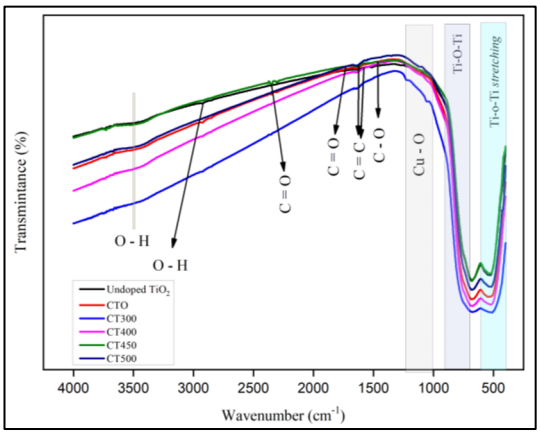

Fig. 4. FTIR results for each sample variation.

The FTIR spectrum for Cu-doped TiO_2 material shown in Figure 4. FTIR testing used to analyze the functional group bonds present in the sample. It also used to indicate the formation of TiO_2 and Cu doping bonds. In the figure, each sample has almost the same absorption band. TiO_2 materials without doping and materials without annealing have bonds as normal Ti – O – Ti without stretching and vibration, namely at wave numbers 677.87 cm-1 and 677.82 cm-1.

Adding Cu doping material resulted in stretching Ti – O – Ti bonds in the CT300, CT400, CT450, and CT500 samples, namely at wave numbers 400 cm-1 to 600 cm-1. The addition of doping shifts the position of the absorption band caused by the insertion of material from the sample lattice [15]. In addition, bond vibrations were observed in the wave number range of 1000 cm-1 to 1250 cm-1 after the existence of Cu doping, which was identified in the form of Cu-O bonds as a result of lattice vibrations of TiO_2 as a result of the presence of doping material [16]. However, the Cu – O bond was not identified in the CT0 sample because there was no annealing process, which resulted in incomplete bond formation.

Another bond of a C – O – C bond only observed in samples with low temperatures, namely CT300 and CT400 at a wave number of around 1150 cm-1. At high temperatures, namely CT450 and CT500, this bond undergoes bond breaking due to temperature. The C – O bond is observed from about 1462 cm-1 to 1479 cm-1. The C=C bond is observed around 1570-1590 cm-1 and at a wavelength of around 1623 cm-1.

The C = O bond is in the range of wave numbers 1728 cm-1 to 1745 cm-1. The peak at wave number around 2920 cm-1 confirmed the presence of OH bonds in the observed sample structure due to the adsorption of water and hydroxyl agents by the material. In addition, O – H bonds also detected in the range of wave numbers 3485 and 3500 cm-1. The increase in temperature removed the C – O – C functional groups and not seen in the CT450 and CT500 samples. In general, variations in annealing temperature did not change the functional groups significantly.

3.4 Structure Analysis

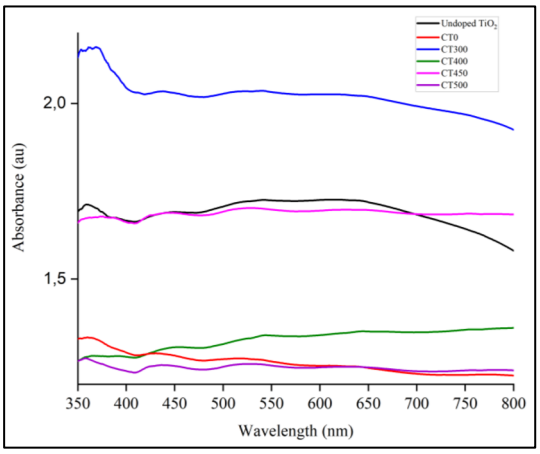

Fig. 5. Absorbance spectra of the photoanode coating each variation

Undoped TiO_2, CT300, and CT400 have absorption in the 350-400 nm region, which is the ultraviolet light region. The undoped photoanode layer shows an absorbance peak at around 360 nm. In the contrast, materials with Cu doping that treated with low-temperature annealing (CT300 and CT400) had almost

the same absorption peaks in the range of 350 nm to 400 nm. It is following the research, which stated that adding Cu doping widened the absorption peak up to 400 nm [17]. This absorption shift is due to the charge transfer transition from O 2p to the d state in Cu. Meanwhile, an increase in temperature on CT450 and CT500 causes a decrease in absorbance in the ultraviolet light range.

The lowest absorbance value obtained from the sample with the highest annealing temperature. It shows that adding of Cu doping increases the absorbance intensity, and the absorption range is more expansive, which is optimal with an annealing temperature of 300°C. This result can also attributed to the larger crystal size due to the increase in annealing temperature. The large crystal size reduces the absorbance ability of the resulting photoanode layer.

The data is also processed using the Tauc Plot method to obtain the energy band gap values. The band gap energy value is determined based on the tangent line between the inflection point on the curve and the hv value of the horizontal axis. The value of this band gap energy results from estimation using the Tauc Plot method.

From these results, it found that the energy band gap decreases after the addition of doping because the doping elements have excess electrons will appear as energy donors. Therefore, the energy required for electrons to move from the valence band to the conduction band (band gap) decreases [18].

Table 1. Bandgap energy for each sample.

Sample	Band gap energy (eV)
Undoped TiO_2	2,42
CT0	2,45
CT300	2,27
CT400	2,39
CT450	2,45
CT500	2,54

In this test, the band gap energy test of the dye used also carried out. The band gap value of N719 dye is 2.29 eV. The sample has a bandgap energy that is almost below the bandgap energy of the dye is the CT300 sample. At high temperatures, the band gap energy increases. This trend caused by the phase change from anatase to rutile in CT450 and CT500.

3.5 Electrical Analysis

This parameter tested using current (I) and voltage (V) testing to obtain the I-V curve. The value of the current strength is obtained by following the following equation 2.

$$I = V/R \quad (2)$$

where I is the electric current (Ampere), V represents the electric voltage (Volts), and R is the electrical resistance (Ohms). Based on the J_{sc}-V curve, the value of the fill factor (FF) is defined by the following equation 3.

$$FF = (V_{max} \times I_{max})/(V_{oc} \times I_{sc}) \quad (3)$$

where I_{max} is the photocurrent density (A) and V_{max} is the photovoltage of maximum power output (V). The variable I_{sc} is the short circuit photocurrent (A), and V_{oc} is the open-circuit photovoltage (V).

Overall DSSC performance is generally evaluated based on the efficiency of converting sunlight into electrical energy expressed by equation 4 [19].

$$\eta = (V_{oc} \times I_{sc} \times FF)/P_{light} \quad (4)$$

where:
V_{oc} = open circuit voltage (V)
I_{sc} = short-circuit current density (mA/cm^2)
FF = fill factor value, and
P_{light} = power of incident light (W)

The irradiation carried out with a light intensity of 1000 W/m2. Undoped TiO_2, namely CT0, experienced a significant decrease in efficiency compared to pure materials without doping, which is 0.44% to 0.9%. It duet to Cu-doped TiO_2 material has not formed. After all, there is no heating process on the material.

The highest efficiency value achieved by DSSC with Cu-doped TiO_2 with an annealing temperature of 300°C which was 0.71%. The efficiency value then decreases with increasing annealing temperature. The CT400 sample has an efficiency of 0.14%, CT450 has an efficiency of 0.09%, and CT500 has the lowest efficiency of 0.08%. The relationship curve between voltage and current density shown in Figure 6.

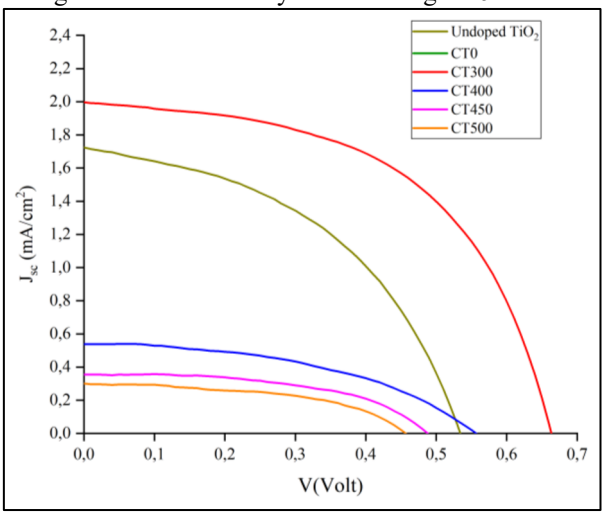

Fig. 6. Voltage curve and Jsc in each sample,

There is an increase in the efficiency of the doped results compared to non-doped materials. However, the efficiency decreased as the temperature of the annealing process increased. These results are also related to the XRD results which show an increasing sample crystal size and the UV-Vis test results, which show that the absorbance ability decreases with increasing annealing temperature.

The highest efficiency found in CT300 sample which showed that an annealing temperature of 300°C was the optimum temperature for the manufacturing of Cu-doped TiO_2. The presence of the anatase phase also affects the performance of DSSC where the anatase phase is the titania crystalline phase which has the best photoactive properties be applied to DSSC.

The anatase phase has a larger particle size so that the surface area becomes larger [20]. Based on the results of the XRD and SEM tests described above, the CT300 sample has an anatase phase without any other

phase and has the smallest crystal size and particle size compared to the other samples. Therefore, the CT300 sample has the most optimal DSSC performance.

4 Conclusions and Recommendations

There is effects of variations in annealing temperature on the structure of the Cu-doped TiO_2 material. Annealing temperature treatments of 300℃ and 400℃ produced the anatase phase without any other phase. Meanwhile, treatment at 450℃ made a mixed phase of anatase and rutile. Samples with an annealing temperature of 500℃ showed a mixture of anatase and rutile phases with more rutile phases. Crystal size increased with increasing annealing temperature. The samples with the lowest to highest temperatures respectively had crystal sizes of 34.82 nm, 35.96 nm, 43.54 nm, and 47.54 nm. The average particle diameter for the non-doped materials, CT300, CT400, CT450, and CT500, respectively, 23.87 μm, 32.54 μm, 33.38 μm, and 37.63 μm.

Functional group bonds were detected as successfully synthesized based on the results of FTIR testing which indicated that the process of making Cu-doped TiO_2 was successful. Photoanode with Cu-doped TiO_2 shows the absorption area in the ultraviolet light region, namely in the wavelength range of 350 nm to 400 nm. Increasing the annealing temperature decreases the absorbance value of the photoanode.

The addition of doping increases the efficiency of DSSC compared to non-doped materials, namely 0.44% to 0.71% in samples with annealing temperatures of 300℃. The CT400 sample has an efficiency of 0.14%, CT450 has an efficiency of 0.09% and CT500 has the lowest efficiency of 0.08%. The efficiency value decreased with increasing annealing temperature. Further research can carried out by BET testing on the surface area of the material which is one of the important factors in DSSC applications. In addition, the hydrothermal method can be used to synthesize of Cu-doped TiO_2.

We thank the Center of Excellence for Electrical Energy Storage, Sebelas Maret University for the research facilities and UMG Idealab for funding for this research and the International collaboration Research grants by Universitas Sebelas Maret, 2023.

References

1. J. Ya'u Muhammad *et al.*, "Recent Progressive Status of Materials for Solar Photovoltaic Cell: A Comprehensive Review," *Sci. J. Energy Eng.*, vol. **7**, no. 4, p. 77, (2019), doi: 10.11648/j.sjee.20190704.14.
2. T. S. Bramhankar *et al.*, "Effect of Nickel–Zinc Co-doped TiO2 blocking layer on performance of DSSCs," *J. Alloys Compd.*, vol. **817**, p. 152810, (2020), doi: 10.1016/j.jallcom.2019.152810.
3. B. Ünlü and M. Özacar, "Effect of Cu and Mn amounts doped to TiO2 on the performance of DSSCs," *Sol. Energy*, vol. **196**, no. December 2019, pp. 448–456, (2020), doi: 10.1016/j.solener.2019.12.043.
4. Z. D. Mahmoudabadi, E. Eslami, and M. Narimisa, "Synthesis of Ag/TiO2 nanocomposite via plasma liquid interactions: Improved performance as photoanode in dye-sensitized solar cell," *J. Colloid Interface Sci.*, vol. **529**, pp. 538–546, (2018), doi: 10.1016/j.jcis.2018.06.048.
5. W. R. Aprilla and A. Haris, "Sintesis Semikonduktor TiO2 serta Aplikasinya pada Dye-Sensitized Solar Cell (DSSC) Menggunakan Dye Indigo Carmine," *J. Kim. Sains dan Apl.*, vol. **19**, no. 3, pp. 111–117, (2016), doi: 10.14710/jksa.19.3.111-117.
6. F. I. M. Fazli *et al.*, "Dye-sensitized solar Cell using pure anatase TiO2 annealed at different temperatures," *Optik (Stuttg).*, vol. **140**, pp. 1063–1068, (2017), doi: 10.1016/j.ijleo.2017.04.027.
7. S. A. Pataya, P. L. Gareso, and E. Juarlin, "Karakterisasi lapisan tipis titanium dioksida (TiO2) yang ditumbuhkan dengan metode spin coating diatas substrat kaca," *Ophthalmology*, vol. **104**, no. 11, pp. 1785–1793, (2016).
8. A. Supriyanto, W. M. Obina, T. Y. Septiawan, A. H. Ramelan, and F. Nurosyid, "Dye-sensitized solar cell (DSSC) performance of copper on TiO2 as a photoelectrode through nanocomposite and electroplating method," *J. Phys. Conf. Ser.*, vol. **1170**, no. 1, (2019), doi: 10.1088/1742-6596/1170/1/012048.
9. T. Raguram and K. S. Rajni, "Synthesis and characterisation of Cu - Doped TiO2 nanoparticles for DSSC and photocatalytic applications," *Int. J. Hydrogen Energy*, vol. **47**, no. 7, pp. 4674–4689, (2022), doi: 10.1016/j.ijhydene.2021.11.113.
10. H. Esgin, Y. Caglar, and M. Caglar, "Photovoltaic performance and physical characterization of Cu doped ZnO nanopowders as photoanode for DSSC," *J. Alloys Compd.*, vol. **890**, p. 161848, (2022), doi: 10.1016/j.jallcom.2021.161848.
11. A. Syukron, D. D. Risanti, and D. Sawitri, "PENGARUH PREPARASI PASTA DAN TEMPRATUR ANNEALING PADA DYE SENSITIZED SOLAR CELL(DSSC) BERBASIS NANOPARTIKEL ZnO," *J. Artik.*, vol. **2**, no. 2, (2013).
12. P. Pandey, M. R. Parra, F. Z. Haque, and R. Kurchania, "Effects of annealing temperature optimization on the efficiency of ZnO nanoparticles photoanode based dye sensitized solar cells," *J. Mater. Sci. Mater. Electron.*, vol. **28**, no. 2, pp. 1537–1545, (2017), doi: 10.1007/s10854-016-5693-9.
13. L. Zhou *et al.*, "Improved performance of dye sensitized solar cells using Cu-doped TiO 2 as photoanode materials : Band edge movement study by spectroelectrochemistry," *Chem. Phys.*, vol. **475**, pp. 1–8, (2016), doi: 10.1016/j.chemphys.2016.05.018.

14. N. M. Safiay, R. A. Rani, N. Ezira, A. Azhar, Z. Khusaimi, and M. Rusop, “Influence of Different Annealing Temperatures on the Structural and Optical Properties of TiO 2 Nanoparticles Synthesized via Sol-Gel Method : Potential Application as UV Sensor,” vol. **21**, no. 2, pp. 279–285, (2021), doi: 10.22146/ijc.52255.
15. T. Raguram and K. S. Rajni, “Synthesis and analysing the structural, optical, morphological, photocatalytic and magnetic properties of TiO2 and doped (Ni and Cu) TiO2 nanoparticles by sol–gel technique,” *Appl. Phys. A Mater. Sci. Process.*, vol. **125**, no. 5, (2019), doi: 10.1007/s00339-019-2581-1.
16. R. Ahmadiasl, G. Moussavi, S. Shekoohiyan, and F. Razavian, “Synthesis of Cu-Doped TiO2 Nanocatalyst for the Enhanced Photocatalytic Degradation and Mineralization of Gabapentin under UVA/LED Irradiation: Characterization and Photocatalytic Activity,” *Catalysts*, vol. **12**, no. 11, (2022), doi: 10.3390/catal12111310.
17. O. P. Choudhary and P. ka, “Scanning Electron Microscope: Advantages and Disadvantages in Imaging Components,” *Int. J. Curr. Microbiol. Appl. Sci.*, vol. **6**, no. 5, pp. 1877–1882, (2017), doi: 10.20546/ijcmas.2017.605.207.
18. J. F. Warman and D. Dahlan, “Sintesis Lapisan Titanium Dioxide dengan Doping Ganda Copper-Silver untuk Aplikasi Fotoanoda Dye Sensitized Solar Cell,” *J. Fis. Unand*, vol. **9**, no. 3, pp. 415–420, (2020), doi: 10.25077/jfu.9.3.415-420.2020.
19. A. Supriyanto, M. I. Darmawan, Hardani, and H. Darmaja, “Fabriksi Dye Sensitized Solar Cells (DSSC) Mengunakan Ekstraksi Bahan-bahan Organik Alam Celosia Argentums dan Lagerstromia sp,” *J. Teknol.*, vol. **9**, no. 3, pp. 1–14, (2013), [Online]. Available: http://onlinelibrary.wiley.com/doi/10.1002/adma.19910030303/abstract.
20. A. P. Winarni, K. Kusumandari, and A. H. Ramelan, “Optimasi Parameter Sintesis Nanopartikel TiO2 untuk Dye Sensitized Solar Cell,” *J. Fis. dan Apl.*, vol. **10**, no. 2, p. 90, (2014), doi: 10.12962/j24604682.v10i2.812.